AJRCCM Articles in Press. Published on June 23, 2005 as doi:10.1164/rccm.200411-1463OC

Fractal Geometry of Airway Remodeling in Human Asthma

[1]Stacey R. Boser, [2]Hannah Park, [3]Steven F. Perry, [4]Margaret G. Ménache and [2]Francis H.Y. Green

1 Dalhousie University, Halifax, Nova Scotia

2 Respiratory Research Group, University of Calgary, Calgary, Alberta T2N 4N1

3 Morphology and Systematics, Institut für Zoologie, Universität Bonn, Poppelsdorfer Schloss, 53115 Bonn, Germany

4 University of New Mexico, School of Medicine, Pediatrics Division, Albuquerque, NM

Request Reprints to: Francis H.Y. Green
Department of Pathology & Laboratory Medicine
3330 Hospital Drive N.W., Calgary AB Canada T2N 4N1
E-mail: fgreen@ucalgary.ca
Fax: (403) 270-8928
Tel: (403) 220-4514

Running title: Fractal Geometry of Asthmatic Airways
Descriptor number: 59
Manuscript word count (excluding abstract): 3441

Supported by the Alberta Lung Association, Health Canada and the Herron Foundation

Copyright (C) 2005 by the American Thoracic Society.

Abstract

Airway wall remodeling is an important aspect of human asthma. In this study fractal analysis was used to provide a relatively simple method for developing a quantitative index of airway wall remodeling in asthmatic and non-asthmatic airways. Negative pressure silicone rubber casts of lungs were made using autopsy material from three groups: fatal asthma, non-fatal asthma and non-asthma control. All subjects were lifelong non-smokers. Non-asthma control casts had smooth walls and dichotomous branching patterns with non-tapering segments. Asthmatic casts showed many abnormalities including airway truncation from mucous plugs, longitudinal ridges and horizontal corrugations corresponding to elastic bundles and smooth muscle hypertrophy, respectively, and surface projections associated with ectatic mucous gland ducts. Fractal dimensions were calculated from digitized images using an information method. The average fractal dimensions of the airways of both the fatal asthma (1.72) and non-fatal asthma (1.76) groups were significantly ($p<0.01$; $p=0.032$, respectively) lower than that of the non-asthma control group (1.83). The lower fractal dimension of asthmatic airways correlated with a decreased overall structural complexity and pathologic severity of disease. This is the first study to use fractal analysis to assess the chronic structural changes of airway remodeling in asthma.

Key words: asthma pathology, airway remodeling, fractal dimension, silicone casts

Abstract word count: 193

Introduction

Remodeling of the airway wall is one of the cardinal features of asthma. It is defined as changes in the composition, content and organization of cellular and molecular constituents of the airway wall (1). Airway remodeling contributes to airway hyperresponsiveness and may lead to a fixed component of airway narrowing (2). Studies of remodeling have provided useful information on tissues obtained at autopsy (3,4) and bronchial biopsy (5,6) and on images obtained by computed tomography (CT) (7,8). These studies have been limited by sample size constraints (bronchial biopsy) or resolution (CT) and have focused on cross sectional changes in the airways. The effects of remodeling on the longitudinal and branching structure of the lung have been relatively neglected.

Euclidean geometry has been the primary tool for describing the conducting airways (length, diameter, branching angles) of healthy adult humans (9,10,11,12). However, Euclidean methods do not provide a measurement indicating the extent of deviation from an idealized tube. This variability is a design feature of the human lung that balances optimal physical structure with physiological robustness (13). Thus, Euclidean methods, while sufficient for describing basic dimensions, are often incapable of generating a precise measure of complex structures such as the bronchial tree, which demonstrate scale independent self similarity with more detail unfolding at higher magnifications (14).

Structures that are irregular and exhibit some form of self similarity are called fractal (14,15,16,17). The degree of such self-repetition can be quantified as a fractal dimension (FD), which is closely related to a power law distribution (16,18). Human

respiration also exhibits fractal fluctuations (19) and fractal models have found new applications in pulmonary medicine. They have been used to quantify breath sounds during exhalation (20), to study the heterogeneity of pulmonary blood flow (21,22) and to quantify low attenuation areas on high resolution CT images from patients with chronic obstructive pulmonary disease (23,24,25). Areas of high and low attenuation will reflect ventilation inhomogeneity due to airway disease. The FD may also be used to describe the space filling ability of a structure; a feature of particular importance to the lung in view of its role in gas exchange (10,26).

Fractal analysis is a relatively simple technique that is well suited to calculate an index quantifying the extent of change in disease states (17). Since FD is a measure of structural complexity (26), we hypothesized that acute asthma would result in a lower overall FD. We report that whole casts of the bronchial trees of both fatal and non-fatal asthma have decreased FD compared to non-asthma controls. This decrease can, in part, be explained by loss of ventilatory units due to bronchoconstriction and mucous plugs. We also found that at higher magnification, individual segments of diseased airways had a higher FD, due to small scale abnormalities associated with airway remodeling.

Materials and Methods

Study Population

The study population consisted of three groups each of six cases: fatal asthma, had asthma and died as a result of it; non-fatal asthma, history of asthma but died of other causes as listed in Table 1; and a non-asthma control, no history of asthma and died of non-respiratory causes. All were lifelong non-smokers; other subject characteristics are listed in Table 1. All had autopsies either through the medical examiner and/or participating hospitals as part of the Prairie Provinces Asthma Study (27). Demographic history, as well as information on asthma, medications, smoking and occupation was obtained from a questionnaire administered to the next of kin and from medical, pharmacy and toxicology records. Further details of group classification are found in references 27 and 28. Consent for autopsy and use of tissues for research was obtained from the families of the deceased. The project was approved by the Conjoint Ethics Committees of the University of Calgary and the University of Alberta.

Pathology

The lungs were fixed with a dual perfusion technique involving cannulation of the pulmonary arteries and major bronchi with 2.5% gluteraldehyde at 20cm H_20 pressure for 24 hours. At autopsy, a pathological assessment of asthma severity was made and a score ranging from 0 (absent) to 3 (severe) was assigned based on histological evaluation of lung sections from upper and lower lobes of the left lung. The overall severity score was based on evaluation of four major histological attributes of asthma: inflammation, mucous gland hypertrophy, airway smooth muscle hyperplasia and thickening of the

subepithelial connective tissues (lamina reticularis) (29). A stratified technique was used to sample axial airways to the apical segment of the left upper lobe and the anterior and basal segments of the left lower lobe. Sections of airways, ranging from cartilaginous bronchi to terminal bronchioles were stained with hematoxylin and eosin and PAS/Alcian Blue for mucous substances. Morphometric analyses of airway smooth muscle and mucous glands were done with a grid and values for mucous glands and smooth muscle were normalized to the internal perimeter of the airway (28). The eosinophilic infiltrates were graded into absent (grade 0), mild (grade 1), moderate (grade 2) and severe (grade 3). Intra and inter observer variability ranged from 2 to 6%. Death from asthma was defined as history of asthma combined with gross and microscopic evidence of asthma with asphyxia (hyperinflation and collapse, mucous plugging, petechial hemorrhages of the serosal cavities and bronchoconstriction). Other potential causes of death were elminated with the use of the medical history, a toxicology profile and full autopsies.

Preparation of Casts

Silicone rubber casts were prepared using a negative pressure injection technique described by Perry *et al*. (30). In order to demonstrate that the casts were true replicas of the airways and to determine the relationship between cast features and airway anatomy and pathology, microdissections were performed on selected lungs prior to bleach digestion (30).

Fractal Analyses

Black and white images of the silicone casts were obtained at a resolution of 1280 X 960 pixels, using a digital camera with constant settings of focal length, shutter speed and aperture size under a constant illumination (AGFA ePhoto 1280). A 'front' and a 'back' image were made of each cast and were edge sharpened by 5%. FD of both images were calculated and averaged for statistical analysis.

FD was calculated using the information method (Benoit 1.1, TruSoft Int'l Inc., St. Petersburg, FL). The black and white images were converted to an outline of single pixels and rotating grids up to 26 squares with side lengths ranging from 1 to 891 pixels were placed over the image. The number of squares containing the outline of the image was counted and weighted (informed) by the proportion of the square including the image. As shown in Figure 1, log-log graphs of the information entropy [I (d)] against the box side length (d) were plotted, yielding a linear relationship with a general equation, $\log[I(d)] \approx -FD \log(d)$. Thus, FD was given as the slope. For some images, no additional information was gained by increasing the box size beyond a certain number of pixels. That is, as d increased, [I (d)] remained constant. Additionally, both the Benoit software and other researchers have strongly suggested that points falling in the lowest and highest orders of magnitude be excluded from the calculation of FD, to compensate for the finite nature of biological structures (31). These points were removed from the calculation of the FD (Figure 1).

To examine the effects of ectatic mucous gland ducts and other surface abnormalities, 10 representative airways from asthmatic casts and 9 representative airways from non-asthma control casts were selected. These airways were isolated by

pulling back the remaining branches from the field of view of the camera when the images were obtained. As before, the images were taken with a constant focal length, lighting, aperture and shutter speed. Prior to downloading the images onto a computer, the images were trimmed using a feature in the camera that allows such a procedure without compromising image resolution. These highly magnified images of an airway were converted into outlines using the Image J software (Image J, Wayne Rasband, Bethesda, MD), and their FD determined using the information method described above.

A sensitivity analysis was performed to examine the effects of complete airway closure on FD. The closures were simulated by sequentially trimming a non-asthma control cast, not used in the previous analyses, in both the number of branches and their length until it consisted only of the major bronchus and a few major branches. Using a non-asthma control cast minimized possible noise from other structural irregularities present in the diseased cases, and ensured that any changes in FD were due to the truncations. The cast was pinned onto a stage to minimize shifting. At each trimmed stage, the number of cuts made was recorded, and an image of the trimmed cast was obtained at a resolution of 2560 X 1920 pixels. The FDs of the images were calculated using the same protocol as indicated above, and plotted against the number of cuts to determine a trend.

Statistical Analyses

For group (fatal asthma, non-fatal asthma, non-asthma control) comparisons of the FD, a one-way analysis of variance (ANOVA) with a Student Newman Keuls test was performed. Effects of eosinophilic infiltrates on FD were studied using a t-test to

compare cases with grades 0 and 1 eosinophilic infiltrates to those with grades 2 and 3 eosinophilic infiltrates. The Pearson correlation test was used to evaluate the linear relationship between asthma duration (years), mucous gland and smooth muscle area and FD. For all tests, a value of $p<0.05$ was considered to be statistically significant. All analyses were performed using SAS software.

Results

Gross Appearances of the Casts and Pathology

Photographs of representative casts from each group are shown in Figure 2. The non-asthma control casts were uniform in diameter along each airway generation, without enlarged mucous ducts or longitudinal ridges (Figure 2A). Close-up views of the smaller airways of the non-asthma control casts revealed considerable detail with filling of individual alveoli arising from respiratory bronchioles (Figure 2B). Casts of the fatal asthma cases were markedly different from the non-asthma control and the non-fatal asthma groups (Figure 2C). A typical fatal asthma cast showed architectural remodeling throughout its length; many segments showed marked tapering, irregular constrictions, longitudinal ridges and surface protrusions (Figure 2D). Truncation of airways due to mucous plugs was a common feature. The non-fatal asthma casts were also abnormal, but to a lesser degree than the fatal asthma casts (Figure 2E). They showed prominent longitudinal ridges and increased surface protrusions, compared to the non-asthma control casts, but lacked the constrictions and segmental tapering characteristic of the fatal asthma group. Microdissections revealed that the surface protrusions corresponded

to ectatic mucous gland ducts. The prominent longitudinal ridges and constricted areas corresponded to hypertrophic longitudinal elastic bundles (29) and smooth muscle bundles (32), respectively on histologic examinations. The results of the morphometric analyses of the airway pathology are given in Table 2.

Fractal Analyses

The FD of the images of the whole casts was significantly lower in both the non-fatal asthma (1.76 ± 0.02) ($p=0.032$) and fatal asthma (1.72 ± 0.02) ($p<0.01$) groups compared to the non-asthma control group (1.83 ± 0.01) (Figure 3). The FD was not significantly different between non-fatal asthma and fatal asthma ($p=0.21$).

The FD was significantly higher ($p<0.01$) for the outlines of the airways with irregular outlines (1.11±0.01) than the outlines of smooth airways (1.02±0.01).

Figure 4 shows the sequential trimming of the non-asthma control cast used to simulate the effects of airway obstruction. Prior to trimming, the FD was 1.79, which is slightly lower than the average FD reported for the six non-asthma control casts used in this study. The value of FD decreased approximately monotonically as the bronchial tree was pruned from 0 – 150 cuts (Figure 4).

There were no statistically significant relationships between FD and age ($r= -0.04$, $p=0.9$), sex ($p=0.7$) or duration of asthma ($r= -0.29$, $p=0.36$). There were significant negative relationships between FD and area of mucous glands ($r= -0.52$, $p=0.03$), and airway smooth muscle area ($r= -0.51$, $p=0.03$). There was no significant difference in FD between the asthmatics of eosinophil grade 0-1, and 2-3 ($p=0.08$).

Discussion

In this study, FDs of silicone rubber casts of airways from asthmatics and control subjects were determined using an information method. A sensitivity analysis was used to illustrate the effect of mucous plugs on FD at a low magnification. Visual examination of these casts showed clear differences between the lungs of subjects who died with or of asthma compared to those who died without asthma and of non-respiratory causes (Figure 2). The most striking feature of the fatal asthmatic casts was the overall loss of airways due to mucous plugs and bronchoconstriction, and this was quantified by a statistically significantly smaller FD than the FD calculated for the non-asthma control casts. In addition, both fatal asthma and non-fatal asthma cases showed severe airway surface abnormalities which corresponded to known features of remodeled airways associated with asthma, including smooth muscle hypertrophy (32), longitudinal elastic bundles (29) and ectatic mucous gland ducts (33). These features, when examined at higher magnifications were associated with an increased FD.

The overall FD was significantly correlated with morphometric indices of asthma severity including mucous gland and smooth muscle hyperplasia, although not with the severity of eosinophil infiltrates or asthma duration. Our results were not confounded by cigarette smoking, which also affects airway structure and function, as only non-smokers were used.

The mean FD (1.84) measured on normal airways in this study was slightly higher than the values for normal human airways (1.75) reported by Kitaoka *et al* (34). This

difference is most likely a result of the type of image, as images of reconstructed airways were used by Kitaoka *et al*., whereas digital images of casts were used in this study.

Our study revealed a change in FD in the presence of disease. The FD of both the non-fatal asthma and fatal asthma groups were significantly lower than the FD of the non-asthma control group but not different from each other. The sensitivity analysis showed that approximately 117 cuts (equivalent to 44% of the cast), each of which simulated an airway closure, were required to cause a decrease in FD equivalent to the average seen in the fatal asthma subjects of this study. The FD thus appeared to accurately track the loss of ventilatory units.

A decrease in FD indicates a loss of complexity and thus a decrease in space-filling ability of these airways, which is clearly evident in the fatal asthma cases. Decreased complexity has been described in other diseases such as a heartbeat that becomes more regular preceding cardiac arrest (35,36). What is also interesting is that the data indicate a similar loss of complexity in the non-fatal asthma cases, although these casts do not appear visually to be as different from the non-asthma control cases as do the fatal asthma cases. Such sensitivity of fractal analysis to detect mild or subclinical disease has been observed in CT studies of patients with COPD (37), but not asthmatic subjects unless they also smoked (38).

Previous Euclidean analyses have demonstrated that although airway lengths and diameters vary considerably, the ratios of their length-to-diameter between generations remain approximately constant (39). These relationships between length or diameter and airway generation are well described by power and multiple exponential functions (9,18,40). It is worth noting that power laws, based on log-log relationships, are thus

related to fractals, suggesting that the value of FD should be consistent with Euclidean models of the normal lung (16,18).

It is argued that many biological structures are not fractal but only space filling, as they are unable to exhibit self-similarity over infinite orders of magnifications (41,42). However, acknowledging the finite nature of biological structures, the airways of the lung follow the definition of a "fractal object" given by Mandelbrot (14), as well as an expanded definition given by Falconer (15) within a limited range of magnification. These definitions are that a fractal structure has a fine structure, is too irregular to be precisely described with Euclidean geometry, exhibits self-similarity, and that it has a FD greater than its topological dimension (15). Thus, describing airway structure with FD is indeed valid.

There are numerous methods to calculate FD, all variants on the basic concept of overlaying objects of decreasing size on an image of a structure, and then counting the number of objects that fall on the surface of the structure. The most commonly used objects are squares although triangles have also been used (43). How an object is measured may have a substantial impact on the resultant FD. As reported by Fernández *et al*., use of a simple box counting method (a box is counted if it touches the structure at all) may result in anomalies not found with a weighted (informed) or sand box counting method (a box is weighted by the proportion that is filled with the structure) (41). Perhaps, the sensitivity of the FD value with regard to the method of measurement is part of the reason why its use in studying diseases such as emphysema has been limited (44). If used, however, as an index of structure or change in structure, the exact interpretation of the meaning of the FD is less important than its ability to discriminate between states.

An advantage of using the information method, which weights each box according to the proportion filled, for calculating FD is that it is less likely to result in a false detection of multifractal characteristics (41). In fact, the presence of more than one fractal structure in an object or multifractal characteristics is common in normal and diseased biologic samples (45). Higher magnification images of the airway segments from asthmatic subjects revealed an increased surface complexity (primarily ectatic mucous gland ducts) associated with remodeling.

To test if these changes would increase the FD, analyses were done on images of isolated airway segments at higher magnification. It was found that the mean FD for asthmatic airways was indeed significantly higher than those without such abnormalities. Since these highly magnified images excluded all other components of the cast such as the branches except for a representative segment, the increase in FD can be attributed to the increase in surface complexity from the airway remodeling.

In diseases such as cancer, morphological complexity may increase (and FD increases) (46). Landini and Rippin reported an increasing FD from normal through dysplastic to cancerous lesion as seen at the interface between the mucosa and connective tissues in the floor of the mouth (47). Thus, the interpretation of FD is complex, as it appears that as physiologic complexity decreases, pathologic complexity may increase.

One may question why the ectatic mucous gland ducts and other irregularities on the airway surface of the fatal asthma cases, which increased surface complexity of the asthmatic airways were not reflected in the overall FD. This is because of the resolution of the images of the bronchial casts, and the exclusion of the lowest order of magnitude of the log-log plots used to calculate FD (see methods and Figure 1). In doing so, the

ectatic mucous gland ducts, whose size ranged between 4 to 9 pixels (380µm to 856µm), were too small to be detected by the smallest box size at 10 pixels (951µm). Consequently, the lower overall FD of the asthmatic lungs reflects only the branching tree structure of the airways and not their surface features.

Thus, an airway tree, like other objects in nature, contains more than one fractal structure and an overall FD does not necessarily provide a complete description of the airways in the diseased lung. Similarly, simple measurements of the length and diameter of an airway do not reflect the roughened surfaces, irregularities or absent functional units, which are often encountered in biological samples and are especially prominent in the lung casts of fatal asthma and non-fatal asthma cases (Figures 2-4) (48). As suggested by Chau (49), use of multiple analytical techniques at appropriate magnifications for the feature of interest are becoming increasingly pertinent to explore the complexity of biological structures.

In summary, our results show that calculation of a FD using an information method for the asthmatic airway provides a rapid assessment of disease relative to a normal lung. It appears from our data that a single measurement of the bronchial tree reflects the severity of disease as determined by pathologic analysis. An improved understanding of airway remodeling in asthma may be important for modeling particle deposition and for improving drug delivery in the asthmatic airways.

Acknowledgements

The authors wish to thank Dr. Robert Cowie and Dr. Richard Leigh for their helpful suggestions in revising the manuscript, Artee Karkhanis for technical assistance and Marnie Cudmore for administrative assistance.

References

1. McParland BE, Macklem PT, Paré PD. Airway hyperresponsiveness: From molecules to bedside Invited review: Airway wall remodeling: friend or foe? *J Appl Physiol* 2003; 95: 426-434.

2. Ward C, Johns DP, Bish R, Pais M, Reid DW, Ingram C, Feltis B, Walters EH. Reduced airway distensibility, fixed airflow limitation and airway wall remodeling in asthma. *Am J Respir Crit Care Med.* 2001; 164(9): 1718-21.

3. Ebina M, Yaegashi H, Chiba R, Takahashi T, Motomiya M, Tanemura M. Hyperreactive site in the airway tree of asthmatic patients revealed by thickening of bronchial muscles. A morphometric study. *Am Rev Respir Dis.* 1990;141:1327-32.

4. James AL, Pare D, Hogg JC. The mechanics of airway narrowing in asthma. *Am Rev Respir Dis.* 1989;139(1):242-6.

5. Saglani S, Malmstrom K, Pelkonen AS, Malmberg LP, Lindahl H, Kajosaari M, Turpeinen M., Rogers AV, Payne DN, Bush A, Haahtela T, Makela MJ, Jeffery PK. Airway remodeling and inflammation in symptomatic infants with reversible airflow obstruction. *Am J Respir Crit Care Med* 2005; 171(7): 722-7.

6. Chakir J, Shannon J, Molet S, Fukakusa M, Elias J, Laviolette M, Boulet LP, Hamid Q. Airway remodeling-associated mediators in moderate to severe asthma: effect of steroids on TGF-beta, IL-11, IL-17, and type I and type III collagen expression. *J Allergy Clin Immunol* 2003; 111(6): 1293-8.

7. Nakano Y, Muller NL, King GG, Niimi A, Kalloger SE, Mishima M, Paré PD. Quantitative assessment of airway remodeling using high-resolution CT. *Chest.* 2002; 122:271S-275S.

8. Niimi A, Matsumoto H, Takemura M, Ueda T, Chin K, Mishima M. Relationship of airway wall thickness to airway sensitivity and airway reactivity in asthma. *Am J Respir Crit Care Med* 2003; 168(8):983-8.

9. Weibel ER. Morphometry of the Human Lung. Heidelberg, Springer-Verlag: New York, Academic Press, 1963.

10. Horsfield K, Cumming G. Morphology of the bronchial tree in man. *J Appl Physiol* 1968; 24:373-383.

11. Schlesinger RB, McFadden LA. Comparative morphometry of the upper bronchial tree in six mammalian species. *Anat Rec* 1981; 199(1):99-108.

12. Raabe OG, Yeh HC, Schum GM, Phalen RF. Tracheobronchial geometry: human, dog, rat, hamster. Tech. Rep. LF-53, Lovelace Foundation for Medical Education and Research, 1976.

13. Mauroy B, Filoche M, Weibel ER, Sapoval B. An optimal bronchial tree may be dangerous. *Nature.* 2004; 427:633-636.

14. Mandelbrot B. The fractal geometry of nature. New York: W.H. Freeman and Company; 1983.

15. Falconer, K. Fractal Geometry: Mathematical Foundations and Applications Second Edition. West Sussex: John Wiley & Sons; 2003.

16. Weibel ER. Fractal geometry: a design principle for living organisms. *Am J Physiol* 1991; 261: L361-L369.

17. Goldberger AL, West BJ. Chaos and order in the human body. *M.D. Computing* 1992; 9(1):25-34.

18. Suki B. Fluctuations and power laws in pulmonary physiology. *Am J Rsepir Crit Care Med* 2002; 166(2):133-137.

19. Fadel PJ, Barman SM, Phillips SW, Gebber GL. Fractal fluctuations in human respiration. *J Appl Physiol.* 2004; 97:2056-2064.

20. Fernández, JA, Ramirez JI, Fernández MG, Manzano JR, Prat JM. Fractal analysis of tracheal sounds during maximal forced exhalation. *Med Sci Monit.* 2004; 10(1): MT14-18.

21. Hlastala MP, Glenny RW. Vascular structure determines pulmonary blood flow distribution. *News Physiol Sci* 1999; 14:182-6.

22. Venegas JG, Galletti GG. Low-pass filtering, a new method of fractal analysis: application to PET images of pulmonary blood flow. *J Appl Physiol.* 2000; 881365-1373.

23. Mitsunobu F, Mifune T, Ashida K, Hosaki Y, Tsugeno H, Okamoto M, Harada S, Tanizaki Y. Low-attenuation areas of the lungs on high-resolution computed tomography in asthma. *J Asthma.* 2001; 38(5):413-22.

24. Uppaluri R, Mitsa T, Sonka M, Hoffman EA, McLennan G. Quantification of pulmonary emphysema from lung computed tomography images. *Am J Respir Crit Care Med* 1997; 156(1):248-54.

25. Madani A, Keyzer C, Gevenois PA. Quantitative computed tomography assessment of lung structure and function in pulmonary emphysema. *Eur Respir J 2001*; 18:720-730.

26. Glenny RW. Heterogeneity in the lung: concepts and measures. In: Hlastal MP, Robertson HT, editors. Complexity in Structure and Function of the Lung. Washington, USA: University of Washington; 1998. p. 571-609.

27. Hessel PA, Mitchell I, Tough S, Green FH, Cockcroft D, Kepron W, Butt JC. Risk factors for death from asthma. Prairie Provinces Asthma Study group. *Ann Allergy Asthma Immunol* 1999; 83(5):362-8.

28. Carroll NG, Perry S, Karkhanis A, Harji S, Butt J, James AL, Green FH. The airway longitudinal elastic fiber network and mucosal folding in patients with asthma. *Am J Respir Crit Care Med.* 2000; 161(1):244-8.

29. Elias JA. Airway remodeling in asthma. *Am J Respir Crit Care Med* 2000; 161:S168-S171.

30. Perry SF, Purohit AM, Boser S, Mitchell I, Green FHY. Bronchial casts of human lungs using negative pressure injection. *Experimental Lung Research* 2000;26:27-39.

31. Fernández E, Jelinek H. Use of fractal theory in neuroscience: methods, advantages and potential problems. *Methods* 2001;24:309-321.

32. Carroll N, Elliot J, Morton A, James A. The structure of large and small airways in nonfatal and fatal asthma. *Am Rev Respir Dis* 1993; 147(2):405-10.

33. Cluroe A, Holloway L, Thomson K, Purdie G, Beasley R. Bronchial gland duct ectasia in fatal bronchial asthma: association with interstitial emphysema. *J Clin Pathol.* 1989; 42(10):1026-31.

34. Kitaoka H, Takahashi T. Relationship between the branching pattern of airways and the spatial arrangement of pulmonary acini: a re-examination from a fractal point of view. In: Nonnenmacher TF, Losa GA, Weibel ER, editors. Fractals in Biology and Medicine. Basel, Switzerland: Birkhauser Verlag; 1994. p. 116-131.

35. Goldberger L, Rigney DR, West BJ. Chaos and fractals in human physiology. *Scientific American* 1990; Feb 43-49.

36. Goldberger AL, Amaral LA, Hausdorff JM, Ivanov PC, Peng CK, Stanley HE. Fractal dynamics in physiology: alterations with disease and aging. *Proc Natl Acad Sci U S A.* 2002; 19;99 Suppl 1:2466-72.

37. Bankier AA, Madani A, Gevenois PA. CT quantification of pulmonary emphysema: assessment lung structure and function. *Crit Rev Comput Tomogr* 2002; 43(6):399-417.

38. Mitsunobu F, Ashida K, Hosaki Y, Tsugeno H, Okamoto M, Nishida K, Takata S, Yokoi T, Mishima M, Tanizaki Y. Complexity of terminal airspace geometry assessed by computed tomography in asthma. *Am J Respir Crit Care Med.* 2003; 167(3):411-7.

39. Nelson TR. Fractals, physiologic complexity, scaling, and opportunities for imaging. *Invest Radiol* 1990; 25:1140-1148.

40. West BJ, Bhargava V, Goldberger AL.Beyond the principle of similitude: renormalization in the bronchial tree. *J Appl Physiol* 1986;60(3):1089-1097.

41. Fernández E, Bolea JA, Ortega G, Louis E. Are neurons multifractals? *J Neurosci Methods* 1999; 89(2):151-7.

42. Avnir D, Biham O, Lidar D, Malcai O. Is the geometry of nature fractal? *Science* 1998; 279(5347): 39-40.

43. Articus K, Brown CA, Wilhelm KP. Scale-sensitive fractal analysis using the patchwork method for the assessment of skin roughness. *Skin Res Technol* 2001; 7(3):164-7.

44. Blundell R, Harrison DJ, Wallace WA. Emphysema: the challenge of the remodeled lung. *J Pathol* 2004; 202(2):141-4.

45. Takahashi T, Murata T, Omora M, Kimura H, Kado H, Kosaka H, Takahashi K, Itoh H, Wada Y. Quantitative evaluation of magnetic resonance imaging of deep white matter

hyperintensity in geriatric patients by multifractal analysis. *Neuroscience Letters* 2001; 314:413-6.

46. Esgiar AN, Naguib RN, Sharif BS, Bennett MK, Murray A. Fractal analysis in the detection of colonic cancer images. *IEEE Trans Inf Technol Biomed.* 2002; 6(1):54-8.

47. Landini G, Rippin JW. Fractal dimensions of the epithelial-connective tissue interfaces in premalignant and malignant epithelial lesions of the floor of the mouth. *Anal Quant Cytol Histol* 1993;15(2):144-9.

48. Sanders H, Crocker J. A simple technique for the measurement of fractal dimensions in histopathological specimens. *J Pathol* 1993; 169:383-385.

49. Chau T. A review of analytical techniques for gait data. Part 1: Fuzzy, statistical and fractal methods. *Gait Posture* 2000; 13(1):49-66.

Figure Legends

Figure 1.

A. Example graph of image used to calculate FD of a non-asthma control cast. The open and closed plots together illustrate the calculation of a single fractal dimension (FD) using a range of box sizes from 1 to 891 pixels. The closed plots indicate the actual information used in the calculation of FD. The remaining plots for box sizes less than 10 pixels and greater than 100 pixels were excluded from the calculations to compensate for the finite nature of biological structures.

B. Example graph of image used to calculate FD of a fatal asthma cast.

Figure 2.

A. Low power photograph of non-asthma control cast of apical segment of left lower lobe. The cast shows characteristic dichotomous branching pattern with smooth parallel sided segments and complete filling to the level of respiratory bronchioles (shown in greater detail in B). C. Cast of 18-year old female who died of asthma (fatal asthma). The cast shows irregular segments with tapering, constrictions, and surface protrusions. The latter corresponded to ectatic mucous gland ducts on histology. Many of the segments are truncated due to airway constriction. Close up of two truncated airways (arrowheads) from same case are shown in D. E. Cast from 33-year old female who had history of asthma but died from drug toxicity. The cast shows some of the changes seen in the fatal asthma in the profiles of the bronchial segments but airway truncation from bronchoconstriction and mucous plugs is much less. Note: Other non-fatal asthma cases (not shown) had greater airway truncation than seen in this case.

Figure 3.

Average fractal dimensions (FD) for the three groups, non-asthma control, non-fatal asthma and fatal asthma. There is a progressive decline in FD from non-asthma control through non-fatal asthma to fatal asthma. The FD of non-fatal asthma and fatal asthma were both significantly different from non-asthma control ($p<0.05$). The FD of fatal asthma was not significantly different from the FD of non-fatal asthma.

Figure 4.

Sequential trimming was performed on a non-asthma control cast, not used in the study, to mimic airway truncation from bronchoconstriction and mucous plugs. The cast was trimmed in 13 steps and FDs were determined. The FDs were plotted against the cumulative number of cuts (bottom right corner). A significant negative correlation ($r= -0.94$, $p>0.05$), was found for the relationship between FD and cumulative cuts.

Table 1. Subject characteristics including age, sex, asthma duration, asthma grade and cause of death

Group	Age	Sex	Asthma Duration (yrs)	Clinical Severity*	Cause of Death
FA	55	F	10	3	Asthma
FA	59	M	6	2	Asthma
FA	18	M	8	3	Asthma
FA	18	F	16	3	Asthma
FA	24	M	20	2	Asthma
FA	20	F	9	2	Asthma
Mean	**32.3**	**n/a**	**11.5**	**2.5**	**n/a**
Range	**18-59**	**n/a**	**6-20**	**2-3**	**n/a**
NFA	29	F	6	2	Intraventricular hemorrhage
NFA	33	F	31	1	Drug toxicity, obesity
NFA	21	M	17	3	Acute Ethanol Toxicity
NFA	23	M	21.5	2	Asphyxia in avalanche
NFA	25	M	5	2	Morbid obesity
NFA	18	F	2	3	Diabetic ketoacidosis
Mean	**24.8**	**n/a**	**13.75**	**2.2**	**n/a**
Range	**18-33**	**n/a**	**2-31**	**1-3**	**n/a**
NAC	50	F	0	0	Leukemia
NAC	21	M	0	0	Motor vehicle accident
NAC	18	F	0	0	Brainstem tumor
NAC	33	M	0	0	Subarachnoid hemorrhage
NAC	29	M	0	0	Seizure disorder
NAC	31	M	0	0	Self inflicted gunshot wound
Mean	**30.3**	**n/a**	**0**	**0**	**n/a**
Range	**18-50**	**n/a**	**0**	**0**	**n/a**

* Based on response to a questionnaire administered to next of kin, which asked:
How would you rate the overall severity of his/her asthma condition?
0: Absent
1: Mild – interferes infrequently with normal lifestyle
2: Moderate – occasionally interferes with normal lifestyle
3: Severe – seriously interferes with normal lifestyle

Table 2. Severity scores for selected pathologic abnormalities

Group	Overall Pathology Grade[1]	Mucous Gland Area[2]	Smooth Muscle Area[2]	Eosinophil Grade
NAC	0	11.9±3.3	3.8±0.4	0
NFA	0.83±0.31	12.7±1.3	6.6±0.8 *	0.5±0.2
FA	3.7±0.3	17.8±3.8	6.8±0.9 *	2.2±0.3 **

[1] 0: None
1: Mild
2: Moderate
3: Moderate to severe
4: Severe

[2] Areas normalized to internal perimeter of airway

* Significantly different from NAC ($p<0.05$)

** Significantly different from NFA ($p<0.05$)

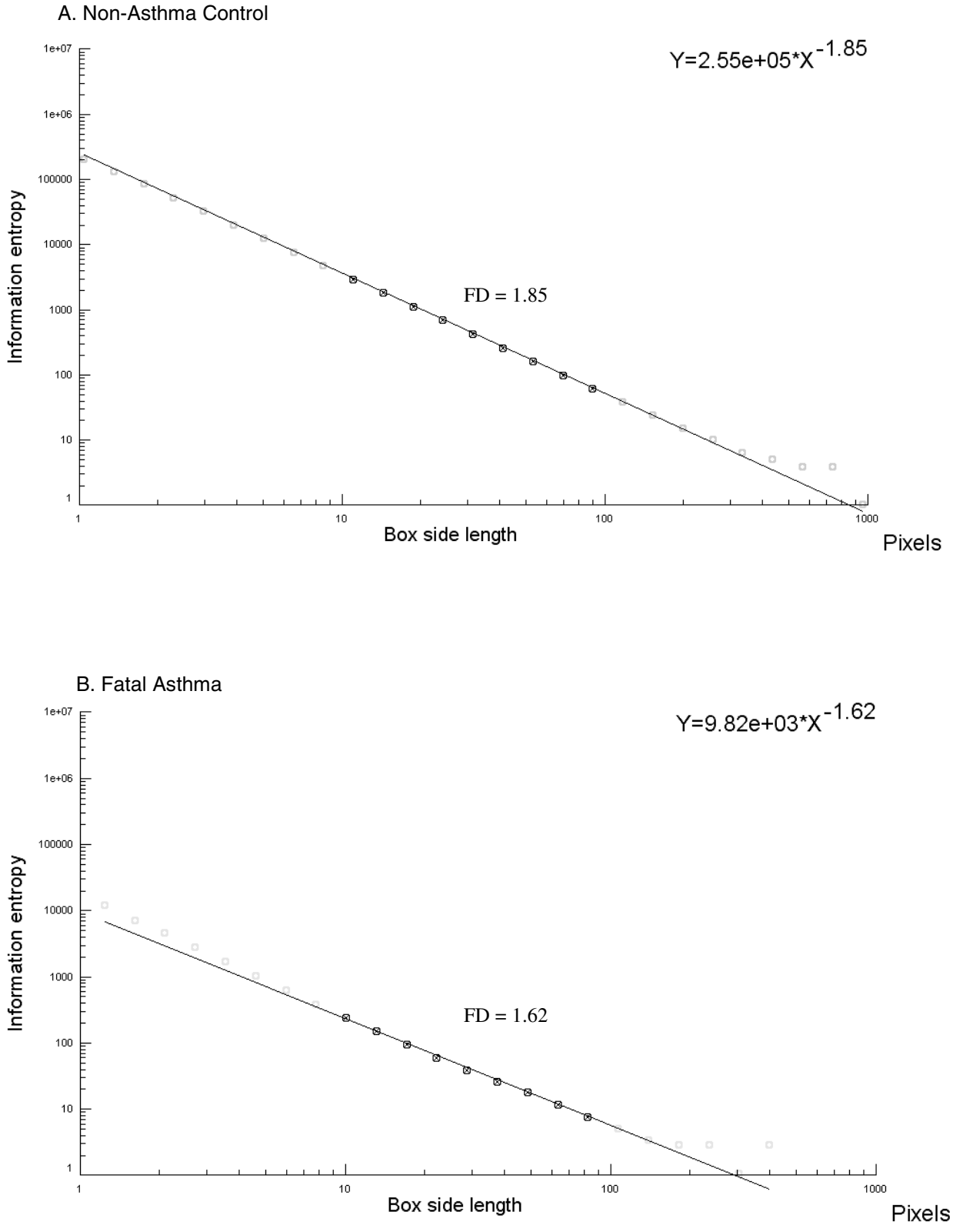
A. Non-Asthma Control
Y=2.55e+05*X^-1.85
FD = 1.85
Information entropy
Box side length
Pixels
1e+07
1e+06
100000
10000
1000
100
10
1
1
10
100
1000
B. Fatal Asthma
Y=9.82e+03*X^-1.62
FD = 1.62
Information entropy
Box side length
Pixels

Figure 1.

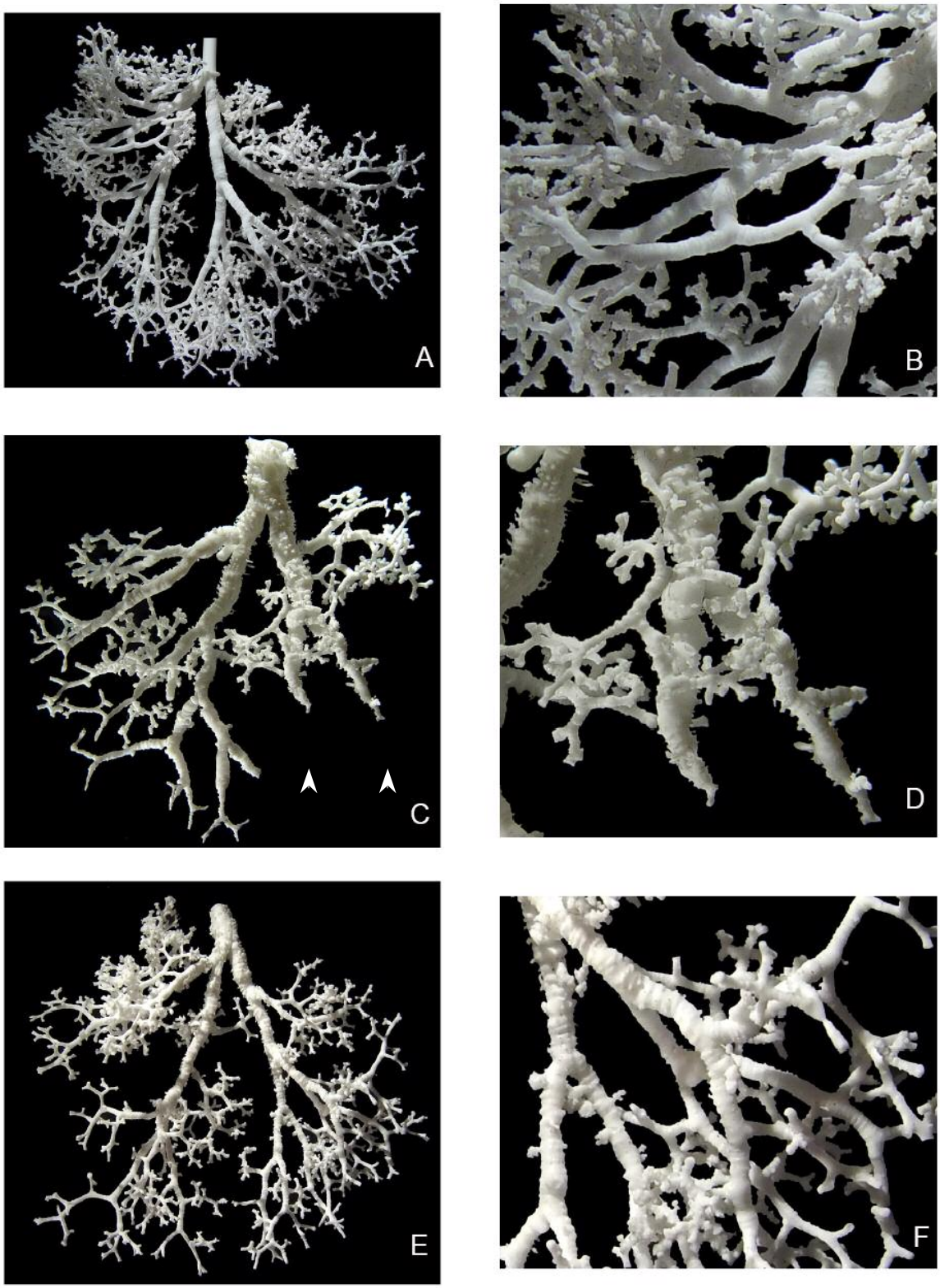

Figure 2.

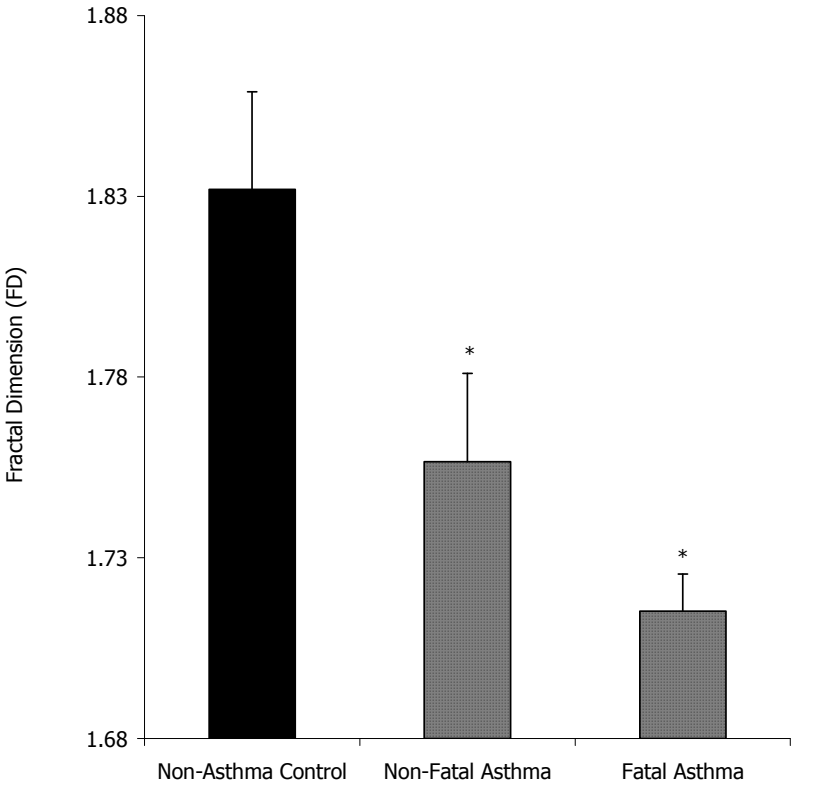

*P<0.05 Fatal Asthma or Non-fatal Asthma vs. Non-asthma Control

Figure 3.

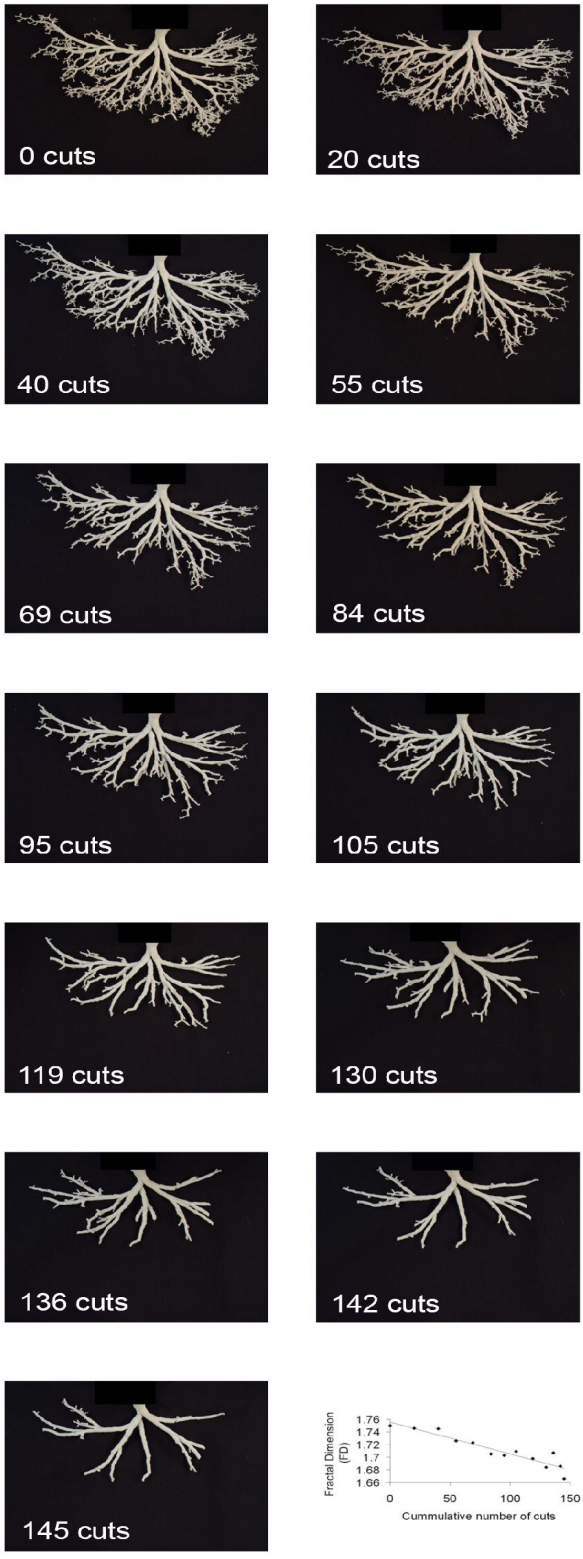
0 cuts
20 cuts
40 cuts
55 cuts
69 cuts
84 cuts
95 cuts
105 cuts
119 cuts
130 cuts
136 cuts
142 cuts
145 cuts
Fractal Dimension (FD)
1.76
1.74
1.72
1.7
1.68
1.66
0
50
100
150
Cummulative number of cuts

Figure 4.